

Contents lists available at ScienceDirect

## Materialia

journal homepage: www.elsevier.com/locate/mtla





## Effective viscous lubrication of cartilage with low viscosity microgels

Ruben J. Trujillo<sup>a</sup>, Acacia T. Tam<sup>a</sup>, Lawrence J. Bonassar<sup>a,b</sup>, David Putnam<sup>a,c,\*</sup>

- <sup>a</sup> Meinig School of Biomedical Engineering, Cornell University, Ithaca, NY, United States
- <sup>b</sup> Sibley School of Mechanical and Aerospace Engineering, Cornell University, Ithaca, NY, United States
- <sup>c</sup> Smith School of Chemical and Biomolecular Engineering, Cornell University, Ithaca, NY, United States

#### ARTICLE INFO

Keywords: Osteoarthritis Ball bearings Lubrication Microgels

#### ABSTRACT

Viscosupplementation is one of the primary treatments for osteoarthritis, with the goal of restoring the viscoelastic properties of native synovial fluid. Recent work shows a strong *in vitro* in vivo correlation between the lubricating abilities of viscosupplements and improved patient reported outcomes, suggesting new viscosupplement formulations need to achieve sufficient lubrication of cartilage to be clinically relevant. This study describes a library of low viscosity microgel suspensions that lubricate cartilage as if they were highly viscous lubricants. Microgel formulations were characterized by their size, rheological properties, and lubricating abilities. Microgels synthesized with low crosslinking density exhibited lubrication equivalent to bovine synovial fluid ( $\mu = 0.037-0.064$ ), while maintaining low measured viscosities similar to PBS ( $\eta(10 \ s^{-1}) = 2.04-4.71 \ mPa*s$ ). These results set the foundation for a new era of viscosupplementation using low viscosity lubricants.

#### 1. Introduction

Osteoarthritis (OA) affects approximately 650 million people worldwide [1,2]. OA is associated with cartilage degradation, joint pain, inflammation, altered synovial fluid content, and negatively affects quality of life [3–6]. Treatment for OA depends on the severity of the disease and includes physical therapy, analgesics, non-steroidal anti-inflammatories (NSAIDs), intraarticular injections of corticosteroids or viscosupplements, and total joint replacement [4,7]. With the exception of total joint replacements, these non-surgical treatment methods only provide short-term pain relief and do not prevent progression of the disease.

Intraarticular (IA) injection of medications are common for OA treatment because they are localized in the joint space which reduces systemic effects [4,8,9]. For example, local injections of corticosteroids reduce inflammation associated with OA. Unfortunately, their effect is short-term due to rapid clearance of small molecules from the joint space [9–11]. Within an articular joint, synovial fluid, comprised of hyaluronic acid, lubricin, and phospholipids, acts as a lubricant and shock absorber [1,4,12]. Viscosupplementation for OA treatment has been used for decades and is based on the importance of synovial fluid, primarily hyaluronic acid (HA), to restore the native viscoelastic properties and lubrication of the healthy joint [4,13–16]. HA viscosupplements

vary in molecular weight, molecular structure (linear versus crosslinked), and concentration, with a general consensus that high molecular weight hyaluronic acid and crosslinked formulations outperform lower molecular weight formulations [4,13,16,17]. The higher molecular weight and crosslinking of HA viscosupplements leads to more viscous solutions that lubricate similarly to native synovial fluid, and notably the viscosity of these formulations exceed that of synovial fluid [13,18]. Different viscosupplements experience variable joint residence times, and have varying biological effects, making the mechanism and duration of therapeutic effects unclear [4,8,19,20]. Lastly, viscosupplements generally require repeated injections and ultimately there is an upper limit to the viscosity, above which the material is no longer injectable [21,22].

While HA therapies have a variety of mechanical and biological effects, recent work shows that lubrication of articular cartilage is highly correlated to positive clinical outcomes [18]. Notably, the effective lubricating viscosity, which differs from bulk viscosity measured by traditional rheological methods, is an excellent predictor of clinical performance. Therefore, the optimum design of next-generation viscosupplements requires molecular architectures that are large enough to be retained in an arthritic joint, have viscosities below the injectable limit, and lubricate articular cartilage sufficiently to impart a clinical benefit. Looking more broadly at the field of lubrication for inspiration,

E-mail address: dap43@cornell.edu (D. Putnam).

<sup>\*</sup> Corresponding author at: Meinig School of Biomedical Engineering, Smith School of Chemical and Biomolecular Engineering, 237 Tower Road, 147 Weill Hall, Ithaca, NY, 14850.

ball bearings are widely used to decrease frictional losses and reduce energy consumption for large equipment, micro-machinery, and more recently for biological lubrication [23–26]. Spherical correlates of ball bearings in the field of drug delivery include liposomes, nanoparticles, and microparticles, which have also been investigated for their lubrication capabilities [27–29]. Liposomes do not have the mechanical integrity to withstand pressures experienced in the joint, and nanoparticles have short residence times due to their size [27]. However, microparticles have prolonged joint residence times relative to smaller particles, making them potential candidates for next-generation IA viscosupplements [10,27,30].

The work herein describes the synthesis and evaluation of a series of spherical micron-sized poly(acrylic acid) hydrogels designed by varying polymer molecular weight and crosslinking density. The microgel library enabled the tuning of microgel size, rheological properties, and lubrication. The microgels exhibited innately low viscosities, yet low crosslinked microgels lubricate articular cartilage in a dose-dependent manner as effectively as synovial fluid and high viscosity lubricants, which have the greatest reported clinical effects. Low bulk viscosities make the microgel formulations easily injectable, while they lubricate at effective viscosities 400–10,000 times higher than those measured by conventional rheology, as demonstrated by large shifts on the Stribeck curve. Notably, we demonstrate that crosslinking density is what ultimately drives lubrication.

#### 2. Materials and methods

#### 2.1. Materials

Anhydrous acrylic acid, tetraethylene glycol (TEG), methoxy poly (ethylene glycol) (mPEG;  $M_n=550~g/mol$ ), Pluronic L35®, 4,4'-azobis (4-cyanopentanoic acid) (A-CPA), 4-cyanopentanoic acid dithiobenzoate (CPA-DB), and potassium bromide (KBr) were purchased from Sigma Aldrich. Dimethyl sulfoxide and methanol were purchased from Fisher Chemical. Neutral aluminum oxide was purchased from J.T. Baker. Biotechnology-grade glycine was purchased from Amresco®. 4-methylmorpholine (NMM) was purchased from BeanTown Chemical. 4-(4,6-dimethoxy-1,3,5-triazine-2-yl)-4-methylmorpholinium chloride (DMTMM) was purchased from Tokyo Chemical Industry. Acrodisc®25 mm syringe filters with 0.8  $\mu$ m Supor® were purchased through Pall Corporation. Phosphate buffered saline (PBS) was purchased from Corning. All chemicals were used as received.

### 2.2. Poly(acrylic acid) synthesis

Poly(acrylic acid) (pAA) was synthesized by reversible additionfragmentation chain transfer (RAFT) polymerization, as previously reported [31,32]. A standard polymerization started with purifying the acrylic acid monomer by removing MEHQ inhibitor in an aluminum oxide column. Appropriate amounts of the CTA (CPA-DB) and initiator (A-CPA) were weighed out depending on the desired molecular weight of the product and placed in a round-bottom flask (see Supplemental). Methanol (40 mL) and the purified acrylic acid (10 mL, 145.85 mmol) were added to the round-bottom flask and the system was purged with nitrogen gas for 15 min to remove excess air. After the removal of air, the round-bottom flask was sealed and then placed in an oil bath at 60 °C. The polymer reaction was quenched in liquid nitrogen after 48 h, a predetermined time where approximately 60 % monomer conversion was expected based on previous experiments [32,33]. A crude sample was taken for proton nuclear magnetic resonance (<sup>1</sup>H NMR, 500 MHz, D<sub>2</sub>O) to determine the conversion of the reaction and the polymer was purified by dialyzing against DI water for three days. Finally, the purified polymer was flash frozen in liquid nitrogen and lyophilized until dry. <sup>1</sup>H NMR was performed on the dried polymer to confirm complete removal of residual methanol, chain transfer agent, initiator, and unreacted monomer. Gel permeation chromatography (GPC) was used

to analyze the polydispersity, weight molecular average, and number molecular average of the pAA.

#### 2.3. Microgel synthesis

Microgels were synthesized using a two-phase microemulsion with DMSO as the dispersed phase and Pluronic L35® as the continuous phase [31]. The carboxylic acid groups on the pAA backbone were condensed with hydroxyl groups on TEG to form a hydrogel network. NMM and DMTMM were used as condensing agents to facilitate the esterification. The total amount of NMM for each reaction differed to achieve different crosslinking densities. pAA (120 mg, 1.67 mmol COOH) was dissolved in DMSO (1.5 mL). DMTMM (276.5 mg, 1.00 mmol DMTMM) and varying amounts of NMM were added to the solution and dissolved with stirring (450 rpm) for 1.5 h. The Pluronic L35® was separated into pre-emulsion (15 g in a glass vial) and homogenization (25 g in a 100 mL beaker) vessels. To the DMSO solution was added TEG (143.8  $\mu$ L, 1.67 mmol of OH groups) and the solution was stirred at 450 rpm for two minutes. The dispersed phase was then pipetted into the pre-emulsion Pluronic L35® vial and vortexed for three minutes to create a homogenous pre-emulsion. The pre-emulsion was then added to the homogenization Pluronic L35® in the beaker (25 g) and the mixture was homogenized at 750 rpm for four hours at room temperature using a Silverson L5M-A Homogenizer with a 1-inch slotted

After the reaction was complete, microgels were pelleted by centrifugation at 9500 rpm at 25 °C for five minutes. The supernatant was decanted using a serological pipette and microgels were resuspended by vortex in 25 mL of DI water. DI water (25 mL) was added to the microgels, followed by sonication (10 min) using a VWR® Ultrasonic Cleaner. Microgels were left suspended in 50 mL of DI water for an additional 20 min unperturbed and at room temperature after the first wash to allow any solvent, Pluronic L35®, and unreacted reagents to diffuse into the water phase. Microgels were subsequently pelleted at 5000 rpm at 25 °C for 5 min. The supernatant was decanted and the microgels were resuspended in 3% w/v glycine (10 mL) and incubated overnight at 4 °C to remove any remaining activated carboxyl groups. Microgels were washed the following day by 3 cycles of re-suspension in 50 mL of deionized water, centrifugation at 5000 rpm at 25 °C for 5 min, and isolated by removing the supernatant. Lastly, microgels were suspended in DI water (5 mL), flash frozen in liquid nitrogen, and lyophilized at room temperature to dryness.

Microgels were additionally synthesized using a syringe pump and syringe filter for studies concerning microgel size dependence and concentration dependence. To do this, the same protocol was followed as described above to form a homogenous pre-emulsion. The pre-emulsion was then added to a 60 mL syringe with a 0.8  $\mu m$  syringe filter and vertically injected into the homogenizing Pluronic L35® using a syringe pump at a rate of 2.5 mL/min. This mixture was then added back to the syringe and filtered an additional two times. After the last filtration, the mixture was left to stir at 250 rpm for 4 h. Microgels were washed in the same manner as described above.

To determine the effect of microgel size on lubrication, microgels of different sizes were separated by differential size centrifugation. Microgels were centrifuged at 1000 rpm at 25  $^{\circ}\text{C}$  for one minute. The supernatant containing the "small" size fraction of microgels was decanted and placed in a separate centrifuge tube. "Small" size fraction and "large" size fraction microgels were centrifuged once more at 5000 rpm at 25  $^{\circ}\text{C}$  for five minutes. Microgels were suspended in 5 mL of DI water, flash frozen in liquid nitrogen, and lyophilized at room temperature to dryness.

#### 2.4. Microgel size analysis

Scanning electron microscopy (SEM) (Tescan Mira3 FESEM) was used to characterize the size and morphology of the microgel

formulations. Conductive double-sided carbon tape was placed on SEM pin stub mounts. Microgel formulations for SEM were prepared via the droplet evaporation technique with microgels suspended in deionized water (0.05–0.1 mg/mL). SEM stubs containing microgels were dried in a desiccator, then sputter-coated with gold and palladium. Microgels were imaged at a working distance of 9 mm at 5 kV. Microgel size was determined using a custom MATLAB code.

Hydrated microgel diameters were acquired by using rhodamine-labeled microgels and confocal microscopy. Low and High XLD microgels were synthesized with 13 kDa pAA in the presence of 0.05 mol% rhodamine6G and washed as described in Section 2.3. Lyophilized microgels were suspended in PBS and the hydrated diameters were measured at pH = 4.5, 7.4, and 9.5 using multi-photon confocal microscope (LSM880 Confocal multiphoton inverted, Zeiss). Images were analyzed using Fiji.

## 2.5. Quantitative and qualitative crosslinking density analysis by <sup>1</sup>H NMR and fourier-transform infrared spectroscopy (FTIR)

Quantitative crosslinking density was determined by replicating the microgel reaction conditions and substituting methoxy PEG (mPEG, containing only one reactive OH group) in place of the TEG crosslinker. pAA (120 mg, 1.67 mmol COOH) was weighed into a glass vial and dissolved in anhydrous DMSO (1.5 mL). DMTMM (276.5 mg, 1.0 mmol DMTMM) and varying amounts of NMM (11 µl, 0.1 mmol for low conjugation; 54.9 µL, 0.5 mmol for medium conjugation; 109.9 µL, 1.0 mmol for high conjugation) were added to the solution and stirred at 450 rpm for 1.5 h at room temperature. After 1.5 h, mPEG (841  $\mu$ L, 1.67 mmol OH) was added to the reaction mixture and allowed to stir for 4 h at 200 rpm. The reaction mixture was purified by dialysis against DI water for at least 3 days and lyophilized to dryness. <sup>1</sup>H NMR was performed on the dried polymer (n = 3) to determine the total conjugation percentage of the mPEG on the pAA backbone. Conjugation percentage was calculated by taking the integral of the -CH3 peak from the mPEG (3.54-3.88 ppm), dividing by 3 to account for the three hydrogens, and finally dividing by the integral of the -CH- backbone from the poly (acrylic acid) (2.22-2.72 ppm).

Qualitative crosslinking density of microgel formulations was determined using FTIR (Bruker Vertex 80v Vacuum System). Three microgel batches with the same molecular weight of pAA and different crosslinking densities were analyzed. KBr was dried overnight in an oven to remove moisture. FTIR pellets (13 mm diameter) were made with 300 mg KBr and 5 mg microgels and compressed to 10 tons with a die kit. Samples were analyzed from  $400~{\rm cm}^{-1}-4000~{\rm cm}^{-1}$  with a resolution of 4 cm $^{-1}$  and 64 total scans. Absorbance data were baseline corrected and normalized to the largest peak.

## 2.6. Rheology

The viscosity of microgel formulations was measured using a commercial rheometer (TA Instruments DHR3 Rheometer). Microgels were suspended in PBS (2.5 mg/mL) and tested using a 40 mm aluminum parallel plate geometry with a 500  $\mu m$  gap width, and a logarithmic shear rate sweep from 1 - 1000 1/s. All tests were conducted at a temperature of 20  $^{\circ} C$  and 10 data points were collected per decade (n=3 per lubricant).

#### 2.7. Friction studies

Friction of various lubricants was measured using a custom-built tribometer, as previously described [18,34–36]. Femoral condyles from the stifle joint of neonatal bovine (Gold Medal Packaging, Syracuse, NY) were harvested and used to make condyle plugs that measure 6 mm wide by 2 mm thick. The cartilage plugs were incubated for 30 min in 1.5 M NaCl in PBS to remove native lubricin from the cartilage surface. The plugs were then incubated in PBS with protease inhibitor

for 1 hour to remove any remaining NaCl. The cartilage plugs were glued to brass pivots and placed in the tribometer wells with the lubricants, compressed to 30 % strain (average contact pressure of  $121\pm29$  kPa), and stress relaxed for 1 hour until they reached an equilibrium normal load. The glass counterface was articulated via a DC motor and the load cells measured the shear force and normal load during sliding. The tribometer platform slid at predetermined speeds ranging from 0.1 mm/s to 10 mm/s.

The friction coefficient was calculated as the ratio of the average shear load while sliding to the average normal load while sliding. All microgel batches were tested at a concentration of 2.5 mg/mL in PBS unless otherwise specified. Bovine synovial fluid (BSF; Lampire) and PBS were used as a positive and negative controls, respectively. Friction data were further analyzed by plotting the friction coefficients versus the Sommerfeld number (Eq. (1)) for PBS and BSF,

$$S = \frac{v\eta_0 a}{F_V} \tag{1}$$

where  $\nu$  is the sliding speed,  $\eta_0$  is the zero-shear viscosity of the lubricant, a is the contact width of the cartilage plug, and  $F_N$  is the normal load of the cartilage plug. A model Stribeck curve was then fit to the PBS and BSF data using (Eq. (2)) for the friction coefficient as a function of the Sommerfeld number,

$$\mu(S) = \mu_{min} + (\mu_B - \mu_{min})e^{-\left(\frac{S}{S_1}\right)^d}$$
 (2)

where  $\mu_{min}$  is the minimum friction coefficient,  $\mu_B$  is the boundary friction coefficient,  $S_t$  is the Sommerfeld transition number, and d is a fitting parameter. The values obtained for the model Stribeck curve are:  $\mu_{min} = 0.046$ ,  $\mu_B = 0.26$ ,  $S_t = 1.81 \times 10^{-7}$ , and d = 0.31. Microgel friction data was plotted as a function of the respective Sommerfeld numbers using the measured viscosity values at  $10~s^{-1}$ .

#### 3. Calculations

#### 3.1. Effective viscosity

The effective viscosity was calculated similar to previous publications with modifications [18,34,35]. For all microgel batches, a custom MATLAB code was used to calculate theoretical Sommerfeld numbers where viscosity values were allowed to vary between  $10^{-6}\,Pa^*s$  and  $10^3\,Pa^*s$  for each experimental sample using Eq. (1). The array of theoretical Sommerfeld numbers was used to calculate theoretical friction coefficients using Eq. (2). Next, the root-mean-square (RMS) error between the experimental friction coefficients and the theoretical friction coefficients was calculated and plotted as a function of viscosity. The effective viscosity was defined as the point where the change in RMS error as a function of viscosity was less than 0.00005.

## 3.2. Theoretical WOMAC score improvements and $EC_{50}$

Average friction coefficients at 10 mm/s were used to extrapolate the theoretical percent change of WOMAC score improvements for  $\rm XLD_{Low}$  microgels at various concentrations based on linear correlations previously published [18]. A variable slope concentration-response model was fit using to the dose dependence microgel friction data at 1 mm/s and used to calculate the effective concentration (EC50) of microgels to decrease friction by half. The bottom plateau was set to be equal to the lowest average friction coefficient.

## 4. Statistics

A two-way ANOVA was used to analyze the average diameters of the microgel batches, aggregated at the picture level, with main effects of crosslinking density, pAA molecular weight, and their interaction. The model assumptions of normality and homogeneous variance were assessed visually using residual plots. Post-hoc pairwise comparisons between batches were performed using Tukey's HSD method to control the Type I error rate. A two-way ANOVA was used to analyze the effects of sliding speed and lubricant on the friction coefficients. A one-way ANOVA was used to analyze the effects of the lubricant on the friction coefficients at an individual speed. Dunnet's multiple comparisons test was performed on MTT data to assess the effects of microgel concentration on cell viability relative to the control. Differences between groups were considered significant at  $p \leq 0.05$  for all statistical tests. All statistical tests were performed using either RStudio or GraphPad Prism.

#### 5. Results

### 5.1. Synthesis of the microgel library

Polymeric microgels, composed of poly(acrylic acid) and tetraethylene glycol (TEG), were synthesized via a two-phase emulsion using DMSO as the dispersed phase and Pluronic L35® as the continuous phase (Fig. 1). For this study, pAA molecular weight and crosslinking density were varied to analyze these parameter effects on microgel properties, leading to the generation of a library of nine distinct microgel formulations (Table 1). The pAA molecular weight and crosslinking density (XLD) used for a specific microgel batch is denoted as pAA<sub>X</sub> where 'X' represents the respective molecular weight, and XLD<sub>Y</sub> where 'Y' represents either low, medium, or high crosslinking density. pAA was successfully synthesized by RAFT polymerization as previously reported by our group [31-33]. RAFT polymerization allows parity between the theoretical and experimental molecular weights, and low polydispersity (D = 1.21-1.31), which were confirmed by both <sup>1</sup>H NMR and GPC (Supplementary Table 1). Microgels were prepared with three distinct pAA number average molecular weights (Mn): 6.9 kDa (pAA<sub>6.9</sub> kDa), 13.0 kDa (pAA<sub>13.0 kDa</sub>) and 22.7 kDa (pAA<sub>22.7 kDa</sub>). These pAA molecular weight targets were chosen to remain below the cut-off for renal filtration (30-50 kDa) [37,38].

Microgel crosslinking density was verified both qualitatively and quantitatively using FTIR and  $^1\text{H}$  NMR for XLD<sub>Low</sub>, XLD<sub>Med</sub>, and XLD<sub>High</sub> microgels. FTIR showed both a decrease in the carboxylic acid peak (O-H stretch between 2500 and 3500 cm $^{-1}$ ) and an increase in the ether peak (C-O-C stretch at 1110 cm $^{-1}$ ) relative to pAA, signifying the incorporation of TEG into the microgels via esterification (Fig. 2A). The decrease in peak signal of the carboxylic acid peak as crosslinking density increases confirms the esterification is taking place, rather than a

Table 1
Three-level two-factor factorial table of microgel formulations varying pAA molecular weight and crosslinking reaction molar ratio. The COOH:NMM ratio represents the molar ratio between the carboxylic acid side chains on the pAA and the NMM.

Microgel Batch		pAA $\overline{M}_n$ (kDa)	Crosslinking Reaction Molar Ratio (COOH:NMM)
pAA <sub>6.9 kDa</sub>	$XLD_{Low}$	6.88	1:0.06
	$XLD_{Med}$		1:0.3
	$XLD_{High}$		1:0.6
pAA <sub>13.0</sub>	$XLD_{Low}$	13.04	1:0.06
kDa	$XLD_{Med}$		1:0.3
	$XLD_{High}$		1:0.6
pAA <sub>22.7</sub>	$XLD_{Low}$	22.70	1:0.06
kDa	$XLD_{Med}$		1:0.3
	$XLD_{High}$		1:0.6

physical mixing of the reactants. Additionally, our lab has previously shown that omission of TEG from the microgel synthesis does not yield microgels or microparticles [31]. Individual FTIR spectra can be found in **Supplementary Fig. 4**. The percent conjugation, used to measure crosslinking density, of XLD<sub>Low</sub>, XLD<sub>Med</sub>, and XLD<sub>High</sub> microgels were 4 %, 12 %, and 15 %, respectively (Fig. 2B), measured via  $^1\mathrm{H}$  NMR through the use of a mPEG conjugation reaction.

To visualize microgel morphology, SEM was used in combination with a custom MATLAB code to determine the average microgel size for each batch. Tuning the microgel crosslinking density led to different sized particles (Fig. 2C). The average diameter was greater for batches with  $XLD_{Low}$  than those with  $XLD_{Med}$  or  $XLD_{High}$  (p < 0.0001). Additionally, for the XLD<sub>Low</sub> batches, the average diameter was greater for the pAA $_{6.9~kDa}$  compared to pAA $_{13.0~kDa}$  or pAA $_{22.7~kDa}$  batches (p <0.0001, Fig. 2D). Dry microgels with  $\mbox{XLD}_{\mbox{\scriptsize Low}}$  had an average diameter between 19 and 28  $\mu m$  while particles with  $XLD_{Med}$  and  $XLD_{High}$  had an average diameter between 5 and 6 µm. Additional data showing the hydrated diameters of Low and High XLD microgels as a function of pH is included in Supplementary Figure 5. Notably, both Low and High XLD microgels swell as the pH transitions from acidic to basic. This transition in swelling state is expected of polyanionic hydrogels as there is a shift in ionization state from a protonated carboxylic acid to a deprotonated carboxylic anion [39].

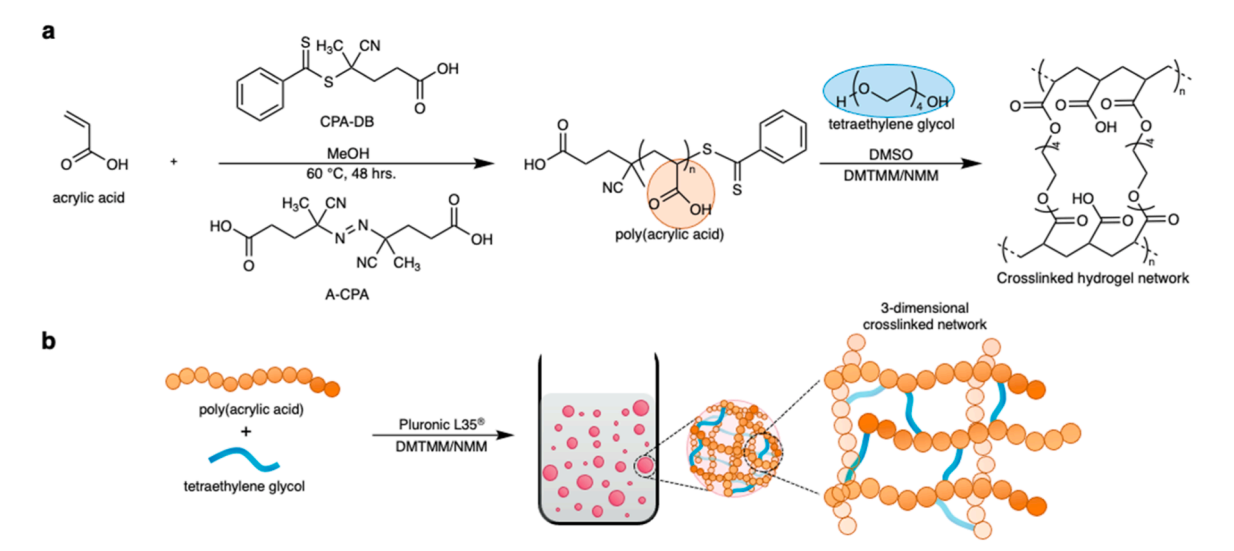


Fig. 1. Microgel Synthesis: a Chemical schematic of the poly(acrylic acid) synthesis using RAFT polymerization and subsequently the microgel synthesis using poly (acrylic acid) and tetraethylene glycol. b Cartoon representation of the microgel synthesis via a two-phase emulsion to produce spherical micron-sized hydrogels.

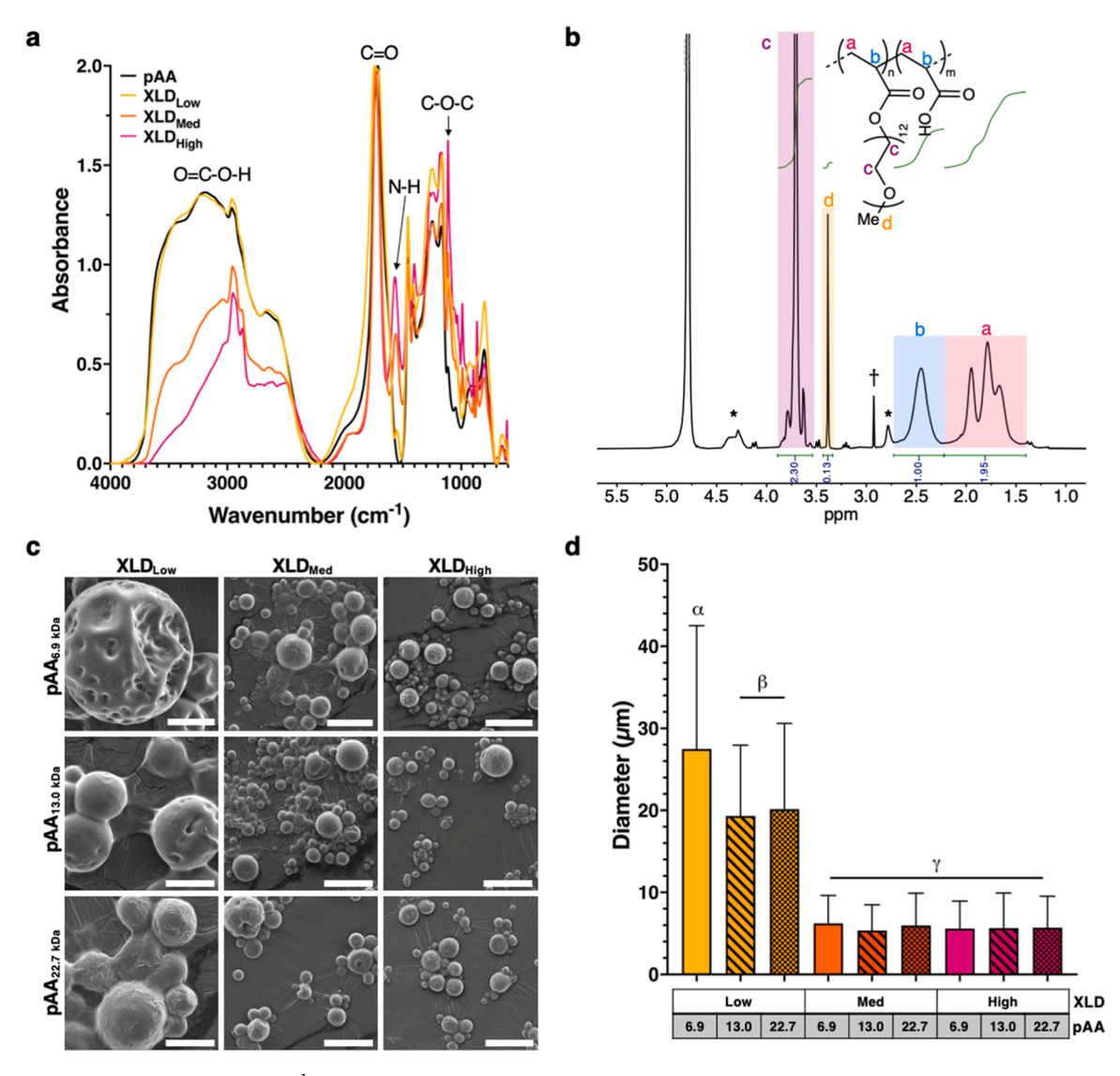


Fig. 2. Microgel characterization: a FTIR and b  $^1$ H NMR were performed to measure the qualitative and quantitative crosslinking density of microgel formulations and pAA-mPEG conjugated polymers, respectively. Peaks denoted with  $^*$  represent the dimerization of the acrylic acid monomer. The peak denoted with  $^\dagger$  represents the methoxy groups found on DMTMM. c Representative SEM images of all microgel formulations (scale bar  $= 20 \mu m$ ) and d average microgel diameters (n = 1236-2733). Statistical significance between groups (p < 0.05) is represented by different symbols.

# 5.2. Polymer microgels achieve high levels of lubrication with low viscosity

Rheology was performed on microgel suspensions (2.5 mg/mL) to determine their viscosity profiles relative to natural synovial fluid and therapeutic HA viscosupplements. Rheological measurements were taken using a parallel plate geometry with a logarithmic shear rate sweep from 1 – 1000 1/s. When comparing the viscosity profiles of microgel suspensions to bovine synovial fluid (BSF) and Hymovis®, an on-market crosslinked viscosupplement (viscosity data obtained from a Carreau-Yasuda model curve)[18], the microgel formulations are 10–1000 times less viscous (Fig. 3A).

Viscosupplementation, as the name suggests, aims to restore the joint's function by providing lubrication through viscosity restoration [4,13–17]. Current on-market viscosupplements have zero-shear viscosity values on the order of 0.5–190 Pa\*s in an attempt to mimic hyaluronic acid, a primary lubricating component of native synovial fluid [18]. Relatively low viscosity values were achieved for microgel suspensions as high as  $10 \text{ mg/mL}(\eta(10 \text{ s}^{-1}) = 4.82 \text{ mPa*s})$ , a concentration comparable to the lower concentrations of viscosupplements [13,40].

Tribological characterization of microgel suspensions was performed on a custom-built tribometer platform to determine the friction coefficients as a function of sliding speed. The results demonstrate that microgel suspensions with low crosslinking density, at all pAA molecular weights, provide low friction ( $\mu = 0.04-0.14$ ) compared to PBS ( $\mu$ =0.19-0.24) and lubricate articular cartilage equivalent to BSF and Hymovis® (Fig. 3B). Additionally, microgel batches with medium and high crosslinking density had friction coefficients equivalent to PBS ( $\mu =$ 0.20-0.23), further confirming that crosslinking density of microgels largely affects lubrication. Microgels synthesized with medium molecular weight pAA and low crosslinking density (pAA13.0 kDa: XLDLow) showed no significant differences in friction coefficients when compared to BSF across all sliding speeds (Fig. S3). Collectively, these data show microgel suspensions used in this study successfully decreased the friction coefficient relative to PBS by as much as 83.5 %, as well as lubricated equivalent to BSF.

## 5.3. High effective viscosities highlight microgel interactions with cartilage

To understand the efficacy of lubrication by microgel formulations,

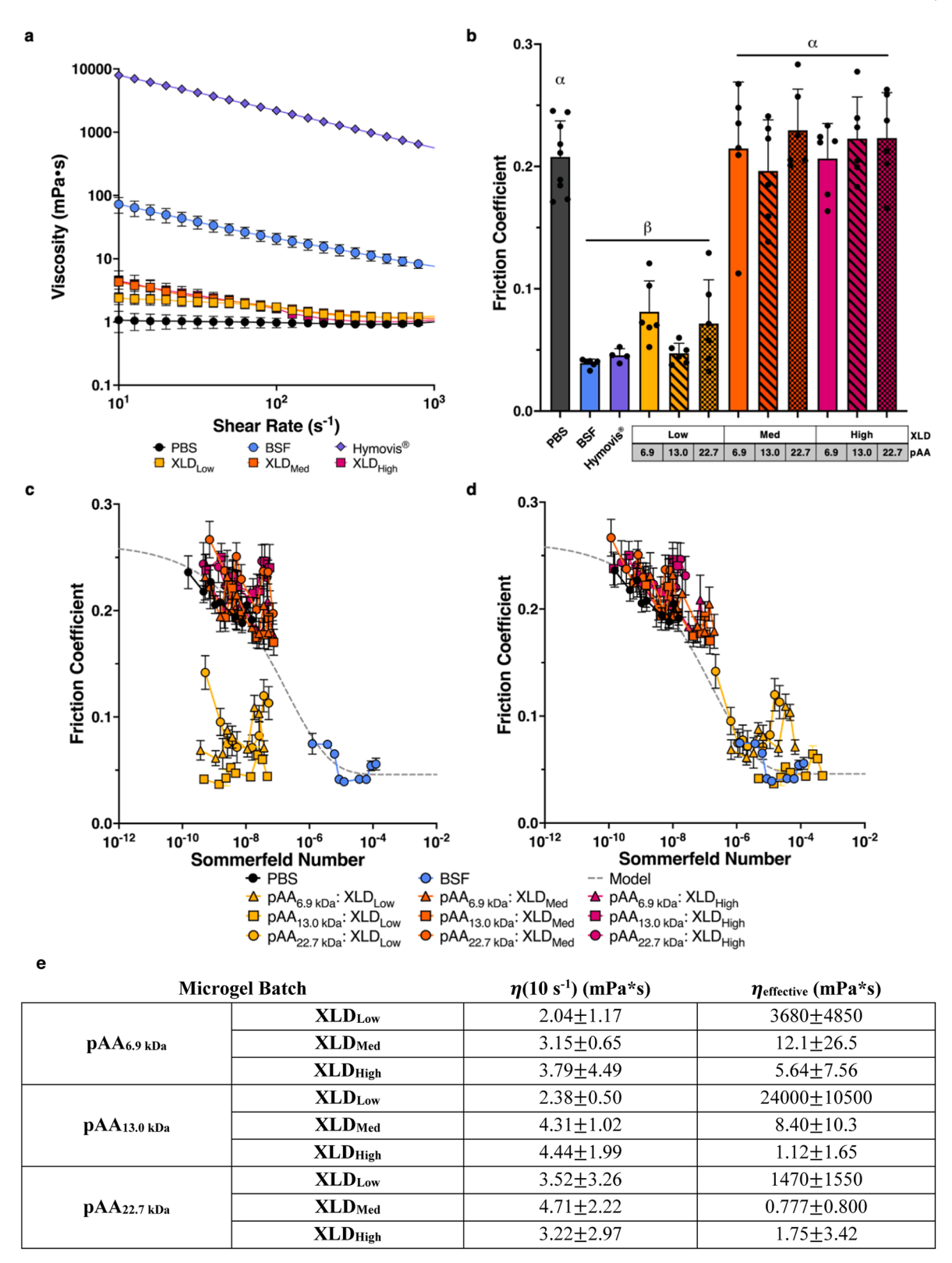


Fig. 3. Rheological and tribological characterization of microgel suspensions: a Viscosity profiles of representative microgel suspensions synthesized with pAA $_{13.0~\text{kDa}}$  are 1–3 magnitudes less viscous than bovine synovial fluid and Hymovis® [18]. Data points are mean  $\pm$  standard deviation (n=1 for Hymovis®, n=3 for PBS, BSF, and microgel formulations). b Friction coefficients of PBS, BSF, Hymovis®, and all microgel suspensions at 1 mm/s. Bar graphs are mean  $\pm$  standard deviation (n=9 for PBS, n=6 for BSF and microgel formulations, n=4 for Hymovis®)[18]; comparisons between groups were conducted using a one-way ANOVA and statistical significance between groups (p<0.05) is represented by different symbols. Stribeck curves of microgel friction data using the c measured viscosity values and d effective viscosity values. Data points are mean  $\pm$  SEM (n=9 for PBS, n=6 for BSF and microgel formulations). e Measured viscosities and effective viscosities of microgel suspensions. Low XLD batches experienced a large increase in effective viscosity while Med XLD and High XLD experienced either a minimal increase or even a decrease in effective viscosity.

we use the Stribeck framework to analyze the friction curves as a function of their respective Sommerfeld numbers. When plotting the microgel friction curves using measured viscosity values, two distinct clusters of data appear (Fig. 3C). Friction curves associated with  $\rm XLD_{High}$  microgels form a cluster towards the mixed mode and boundary mode lubrication regimes, indicating that they do not lubricate well. Additionally, the second cluster that appears is associated with  $\rm XLD_{Low}$  microgels that lubricate exceptionally well. Notably, they do not fall on the model Stribeck curve because their Sommerfeld numbers are too low for their respective friction coefficients due to their low bulk viscosities. Thus, based on classical lubrication theory, this cluster of lubricating microgels would be expected to have higher viscosities based on their unique lubricating abilities.

To better understand the high lubricating abilities of these low viscosity microgel suspensions, a technique that was previously characterized for HA polymer lubricants and inflammatory synovial fluids was

used to show that the lubricating ability does not necessarily map to measured viscosity, but rather to the ability to shift the position on the Stribeck curve. To assess this shift, we used a modified Stribeck framework that determines the effective lubricating viscosity by fitting friction data to the model Stribeck curve (Section 3.2) [18,34]. Using this methodology, large shifts of Sommerfeld numbers were revealed for microgel formulations (Fig. 3D). Specifically, XLD<sub>Med</sub> and XLD<sub>High</sub> batches had low effective viscosities and were generally shifted to the boundary mode lubrication regime. Contrastingly, XLD<sub>Low</sub> microgels formulations exhibited effective viscosities 100–10,000 times larger than bulk viscosities measured by rheology, resulting in a shift to larger Sommerfeld numbers that populate the model Stribeck curve in the mixed mode and elastoviscous lubrication regime (Fig. 3E).

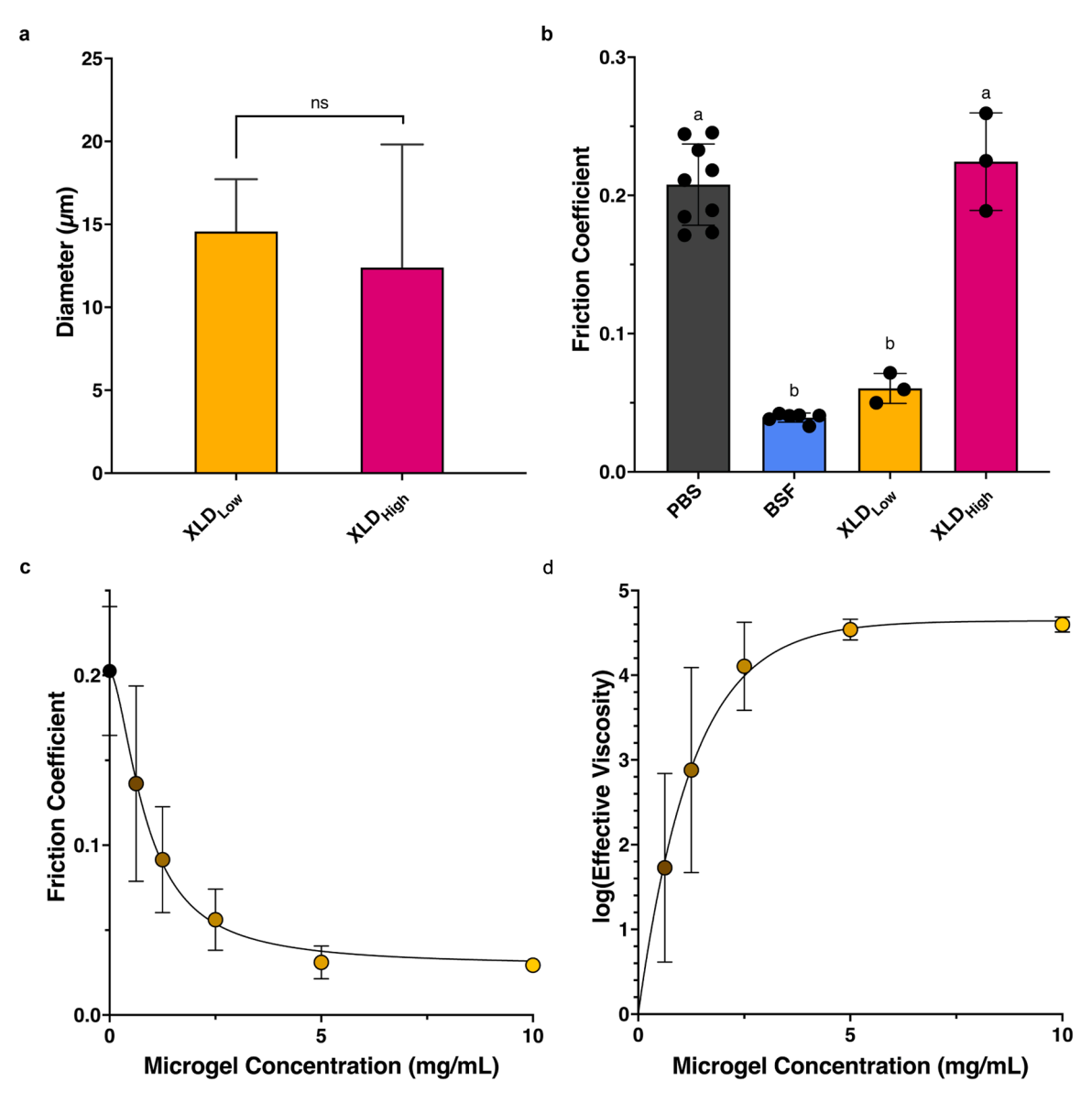


Fig. 4. Effects of microgel size, crosslinking density, and concentration on lubrication. a Average microgel diameter of XLD<sub>Low</sub> and XLD<sub>High</sub> microgels. Bar graphs are mean  $\pm$  standard deviation (n=527 and n=553 for XLD<sub>Low</sub> and XLD<sub>High</sub> respectively). b Friction coefficients of PBS, BSF, XLD<sub>Low</sub> microgels, and XLD<sub>High</sub> microgels at 1 mm/s. Bar graphs are mean  $\pm$  standard deviation (n=9 for PBS, n=6 for BSF, and n=3 for XLD<sub>Low</sub> microgels and XLD<sub>High</sub> microgels); comparisons between groups were conducted using a one-way ANOVA and statistical significance between groups (p<0.05) is represented by different letters. c Friction coefficients versus microgel concentration for XLD<sub>Low</sub> microgels at 1 mm/s. Data points are mean  $\pm$  standard deviation (n=9 for PBS and n=3 for XLD<sub>Low</sub> microgels at all concentrations); comparisons between groups were conducted using a one-way ANOVA. d Log(effective viscosity) versus microgel concentration for XLD<sub>Low</sub> microgels. Data points are mean  $\pm$  standard deviation (n=3 for XLD<sub>Low</sub> microgels at all concentrations).

## 5.4. Elucidating the effects of microgel crosslinking density, size, and concentration on cartilage lubrication

To investigate whether lubrication was dictated by microgel size or by crosslinking density, microgels of similar sizes were synthesized with low and high crosslinking density (Fig. 4A). When the lubrication characteristics of similar sized microgels were evaluated, microgels with XLD<sub>Low</sub> continued to exhibit superior lubrication compared to XLD<sub>High</sub> (Fig. 4B). The dose dependence of lubrication of articular cartilage was evaluated using  $XLD_{Low}$  microgels. Microgels with  $XLD_{Low}$  and an average diameter of 22.5  $\pm$  3.1  $\mu m$  (mean $\pm$ SD, n=6 batches) were evaluated at concentrations varying from 0.625 - 10 mg/mL. Lubrication using XLD<sub>Low</sub> microgels followed a dose dependent response and lubricated equivalent to BSF across all sliding speeds beginning at 2.5 mg/mL, while still maintaining low viscosity values ( $\eta(10 \text{ s}^{-1}) = 4.82$ mPa\*s at 10 mg/mL) (Fig. 4C). The calculated EC<sub>50</sub> was 0.86 mg/mL (R<sup>2</sup>=0.8471) after fitting the microgel dose dependence data at 1 mm/s using a variable slope concentration-response model. Recently, clinical outcomes for viscosupplements, specifically WOMAC scores, were found to strongly correlate to both friction coefficients and effective viscosities [18]. Based on these data, the theoretical percent change of WOMAC score improvements for XLD<sub>Low</sub> microgels at various concentrations were extrapolated to predict the theoretical clinical impact. Using the average logarithmic values of effective viscosity (Fig. 4D), XLD<sub>Low</sub> microgels were calculated to have theoretical WOMAC score improvements between 34.9  $\pm$  6.6 % and 51.9  $\pm$  0.5 % due to their lubrication characteristics (Supplemental Table 2).

#### 6. Discussion

The choice of pAA and TEG for the microgel synthesis was based on their biocompatibility, facile post-polymerization conjugation via the carboxylic acid groups on pAA, and the potential for post-synthesis therapeutic cargo loading, which bypasses relatively harsh reaction conditions [31,41–45]. The microgel synthesis is composed of multiple parameters that could ultimately affect the microgel sizes, viscosity profiles, and lubrication. These parameters include pAA molecular weight, crosslinking density, crosslinker length, type of crosslinker, and emulsification technique. Of these parameters, the most pertinent parameters to evaluate were the pAA molecular weight and crosslinking density of the microgels. It is well established that the viscosity of polymeric solutions varies with polymer molecular weight due to chain entanglement, potentially affecting the viscosity of microgel suspensions [46–48]. Additionally, the crosslinking density of the microgels will directly affect the mesh size, swelling ratio, and the number of free pAA carboxylic acid groups [49–51]. Using a mPEG conjugation reaction, the conjugation reaction efficiency was found to be non-linear with the reaction showing a plateau for the  $XLD_{Med}$  and  $XLD_{High}$  microgels, which is consistent with the relevant DMTMM:NMM synthesis literature [31,45]. Additionally, FTIR, <sup>1</sup>H NMR, and SEM data collectively show non-linear reaction efficiency as XLD<sub>Med</sub> and XLD<sub>High</sub> microgels demonstrate similar FTIR traces, conjugation efficiencies, and microgel size that vary compared to XLD<sub>Low</sub> microgels.

The viscosity of synovial fluid, primarily due to hyaluronic acid (HA), contributes considerably to its lubricating and shock absorbing properties. Within native synovial fluid, hyaluronic acid concentrations vary from 2.5–4 mg/mL, while viscosupplements are more concentrated to achieve highly viscous solutions [4,13,20,52]. Microgel suspensions, at comparable concentrations of native hyaluronic acid in synovial fluid, had viscosity profiles similar to PBS (~1 mPa\*s), independent of the crosslinking density and pAA molecular weight. These microgel suspensions were 10–1000 times less viscous than traditional viscosupplements and bovine synovial fluid, which ultimately requires a lower injection force when compared to viscous counterparts [22]. Similar studies of polymer nanospheres, hyaluronic acid microgels, and biodegradable mesoporous silica nanoparticles (MSNs) demonstrated

similar results for viscosity profiles, in solutions with comparable particle densities between 1 and 20 mg/mL [53–56]. The rheological results for this study also correspond to empirical equations by Einstein, Batchelor, and Krieger and Dougherty, that describe the viscosity of particle suspensions as a function of volume fraction, which only lead to a large increase in viscosity at high volume fractions [57–60].

Microgel suspensions, specifically XLD<sub>Low</sub> microgels, decreased friction of articular cartilage explants relative to PBS up to 83.5 %. A variety of materials and viscosupplements demonstrate lubricating efficacy for articular cartilage. Nanoparticle suspension systems showed a decrease in friction by 30-71.2 % relative to DI water/PBS [53,55,61, 62]. A reduction in friction compared to DI water/PBS was observed between 29.6-50 % in micron-sized suspension systems [28,63,64]. Additionally, numerous synthetic polymers were tested as potential viscosupplements. Polyglycerol dendrimers with low viscosity lubricated cartilage statistically equivalent to BSF and PBS [65]. Lubrication of articular cartilage was also observed for modified hyaluronic acid [66], hyaluronic acid mimetic polymers[67], and lubricin mimetic polymers[68], decreasing friction relative to PBS between 60.8–77.5 %. A more recent study showed crosslinked poly(acrylamide) improved friction by 35-40 % compared to PBS using mechanically impacted and biochemically degraded cartilage explants [69]. XLD<sub>Low</sub> microgel suspensions successfully lubricate articular cartilage and outperform previous nanoparticle, microparticle, and polymeric systems.

Friction data for microgel suspensions, PBS, and BSF, was plotted as a function of the Sommerfeld number (Eq. (1)), which is a function of the lubricant viscosity ( $\eta_0$ ), sliding velocity (v), sample contact width (a), and the applied normal load (F<sub>N</sub>). In the field of tribology, Stribeck curves are used to distinctly map lubrication modes and provide insight on the mechanisms of lubrication [18,34,35]. Although originally developed for hard impermeable materials, multiple groups, including ours, have shown that this framework appropriately describes the frictional behavior of cartilage [18,36,65,67,70-75]. For these tribometric studies, the contact width, normal load, and sliding speed are consistent across all samples, with the viscosity being the only variable that differs across lubricants (microgel suspensions, PBS, and BSF). Based on previous work [18,34-36,73,74], a model Stribeck curve was created by fitting the PBS and BSF friction data using Eq. (2), to obtain the minimum friction coefficient ( $\mu_{min}$ ), the boundary friction coefficient ( $\mu_{B}$ ), the Sommerfeld transition number (St), and the fitting parameter (d) that controls the slope of the transition between lubrication modes. Generally, solutions that achieve remarkable lubrication possess higher viscosities (e.g. HA, pAAm, dextran) [18,36,69]. However, microgel suspensions with low measured viscosity values, exhibited similar lubrication that is theoretically represented by viscous solutions, deviating from classical Stribeck behavior. These deviations indicate unique lubricant interactions at the cartilage interface, leading to friction curves that are shifted relative to the model Stribeck curve [18,34]. More specifically, such deviations suggest that these materials interact with cartilage in a way that makes them more viscous at the cartilage interface, improving lubrication. The discrepancy from classic behavior derives from the realization that conventional rheology measurements conducted with steel surfaces do not accurately reflect viscosity measurements of lubricants conducted at cartilage surfaces. In fact, viscosity values measured between cartilage surfaces for materials such as HA, which are known to interact with cartilage, are 10-20 times larger than measurements made between steel surfaces [48]. In previously reported studies, various on-market HA viscosupplements were evaluated using rheological and frictional techniques [18,76]. The results demonstrated that although these HA formulations had large differences in their dynamic viscosity profiles, frictional performance was not directly correlated to rheological properties based on classical Stribeck curve behavior, suggesting that frictional performance of HA viscosupplements is more complex than conventional rheological measurements. Large differences between measured and effective viscosities in the current study suggest that microgels with low crosslinking density interact with the cartilage surface during sliding, resulting in increased viscosity at the cartilage interface.

Microgel batches with low crosslinking density successfully lubricated cartilage, but they were also significantly larger than medium and high crosslinking density microgels. To elucidate whether microgel suspensions lubricated as a function of size or crosslinking density, lubrication experiments were performed with microgels of the same size, as measured by SEM, but different crosslinking densities. From these experiments, these data confirm that microgel suspensions lubricate as a function of crosslinking density, independent of microgel size. Although crosslinking density is the parameter being modified for microgel formulations in these studies, this directly impacts an array of parameters that need to be considered (Fig. 5). For hydrogels on the macro-scale, as crosslinking density increases, mesh size decreases (d<sub>pore</sub>), which ultimately affects the degree of swelling (R<sub>H</sub>), the amount of crosslinker incorporated, and the mechanics (Young's modulus, E). On the micro-scale as crosslinking density decreases for the microgel formulations, there are more available carboxylic acid groups (degree of ionization,  $\alpha$ ) to interact with the aqueous environment, and it is possible this interaction contributes to lubrication through a hydration lubrication mechanism [1,77]. Additionally, changing the number of free carboxylic acid groups and incorporation of tetraethylene glycol impacts the counterion interactions (osmotic pressure,  $\Pi$ ) and bound water association with the polymer matrix. Generally, hydrogel lubrication is thought to result from high solvent swelling and can occur through mechanisms that involve hydrodynamic forces of fluid flow through the hydrogel network, absorption or repulsion between the gel and the opposing substrate, and micromechanical and thermodynamic properties of the hydrogel network [78,79]. Hydrogels with larger mesh sizes generally have lower friction coefficients, supporting these findings that microgels with low crosslinking density (larger mesh sizes) have improved lubrication over microgels with medium and high crosslinking density [78]. Future work will look at deconstructing the complexities of lubrication as a function of crosslinking density to elucidate the mechanism of action for lubrication.

Current viscosupplement formulations consist of hyaluronic acid concentrations varying from 8 to 22 mg/mL and generally require repeated injections [40]. Lubrication of microgel suspensions as a function of concentration would inform proper doses for an optimum microgel treatment to achieve sufficient joint lubrication equivalent to

synovial fluid. Notably, microgels achieved lubrication equivalent to BSF across 4X dilution and relatively low weight percent (maximum 1 wt/v%) compared to other systems. Similar dose dependence on friction is known for other lubrication systems such as nanosphere suspensions, functionalized mesoporous silica nanoparticles, and lubricin mimetic polymers [29,53,55,68]. Small molecule drugs, proteins, and large molecules, such as hyaluronic acid, have short half-lives within the joint space which are further decreased by the onset of osteoarthritis [4,10, 13,20,80]. In an effort to increase joint residence time for prolonged treatment, multiple studies have shown that micron-sized particles possess increased residence time *in vivo* compared to smaller suspension systems due to their size [10,14,21,27,30]. These studies point to the effectiveness of a microgel treatment across a wide range concentrations that could last throughout multiple half-lives.

As previously noted, HA viscosupplements vary in molecular weight, concentration, and molecular structure, ultimately varying the physical and chemical properties. Although viscosupplements are widely used for osteoarthritis treatment, clinical impact widely varies [8,81]. Due to the wide range of clinical outcomes for HA viscosupplements, determining which factors lead to patient improvement remains difficult. Previous data has shown a strong *in vitro-in vivo* correlation relating patient reported WOMAC scores to both the friction coefficient and effective viscosity of on-market viscosupplements. Using this correlation data, we calculated theoretical WOMAC score improvements as high as 53.4 % (Supplemental Table 2). These data suggests pAA-TEG microgels would improve patient outcomes across a wide range of concentrations, highlighting the clinical significance of pAA-TEG microgel suspensions as an alternative to traditional viscosupplementation.

#### 7. Conclusions

The objective of this study was to generate a library of pAA-TEG microgels and determine the effects of pAA molecular weight and crosslinking density on microgel size, rheological properties, and lubricating abilities. The results presented in this manuscript lay the foundation for microgels as a potential therapeutic for OA treatment. This is the first work, to our knowledge, that characterizes rheological properties and demonstrates the successful lubrication of articular cartilage with pAA-TEG microgels. Using the nine unique combinations of microgel formulations, we studied the effects of pAA molecular

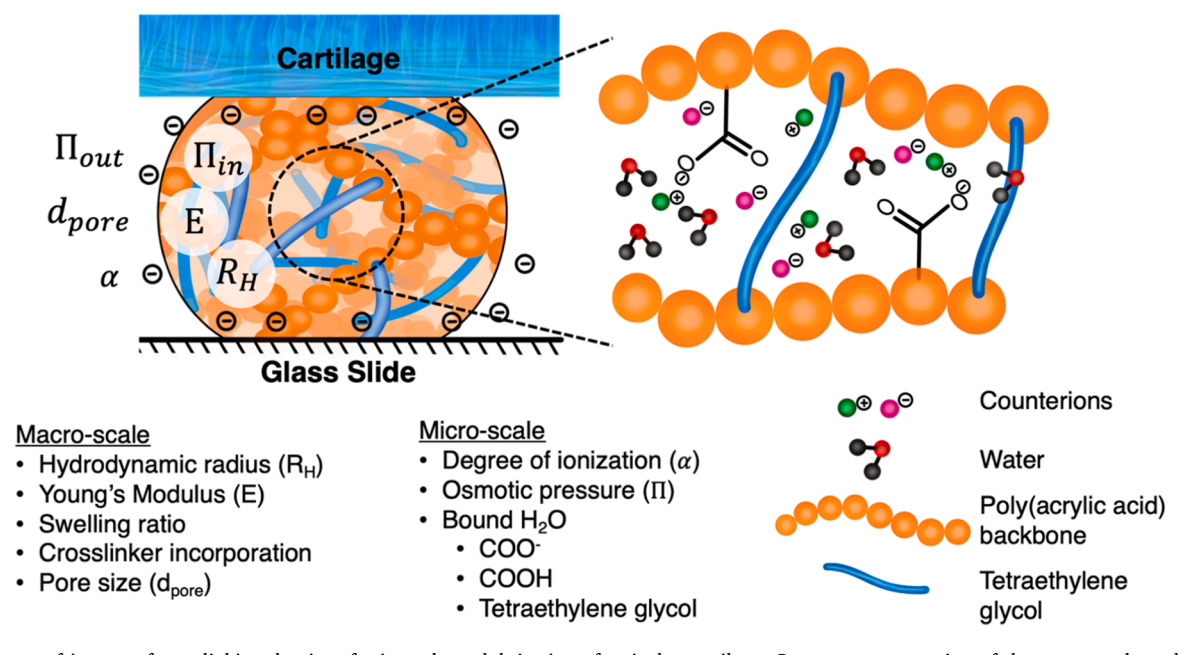


Fig. 5. Diagram of impact of crosslinking density of microgels on lubrication of articular cartilage. Cartoon representation of the macro-scale and micro-scale parameters that are affected by changing crosslinking density of microgel formulations.

weight and crosslinking density on microgel size, viscosity, and lubrication. From these data, it is clear that crosslinking density directly affects microgel size and lubrication. Stribeck curve analysis shows that when classic rheology is used to measure bulk viscosity, these microgel suspensions do not exhibit differences, but when using the effective viscosity, the low crosslinking density microgels experience a dramatic increase in the Sommerfeld number, suggesting that there is an interaction between the microgels and the cartilage surface. Regardless of pAA molecular weight, low crosslinking microgel suspensions exhibited superior lubrication compared to high crosslinking microgel suspensions and lubricated articular cartilage equivalent to BSF. Based on previous work, the level of lubrication achieved here is expected to have a significant clinical impact based on predicted WOMAC score improvements. These data lay the foundation for pAA-TEG microgels as a potential therapeutic for osteoarthritis treatment through lubrication of articular cartilage.

## **Author contributions**

R.J.T, L.J.B., and D.P. designed the experiments. R.J.T. synthesized poly(acrylic acid), synthesized microgels, performed <sup>1</sup>H NMR, FTIR, SEM, and rheological experiments, and performed lubrication studies. R. J.T., A.T.T., L.J.B., and D.P. analyzed and interpreted the data. R.J.T. drafted the manuscript. R.J.T., A.T.T., L.J.B., and D.P. edited the manuscript. All authors have read and approved the final submitted manuscript.

#### **Declaration of Competing Interest**

The authors declare the following financial interests/personal relationships which may be considered as potential competing interests: Putnam and Bonassar hold patents that are currently licensed to entities with potential interest in this research. Neither Putnam nor Bonassar hold equity or have any financial interest in any company that has licensed their patents in this area of research.

### Acknowledgments

These studies were funded by the NSF-GRFP DGE – 2139899 (R.J.T.). The authors acknowledge the use of facilities and instrumentation supported by NSF through the Cornell University Materials Research Science and Engineering Center DMR-1719875. This work made use of the Cornell University NMR Facility, which is supported, in part, by the NSF through MRI award CHE-1531632.

## Supplementary materials

Supplementary material associated with this article can be found, in the online version, at doi:10.1016/j.mtla.2023.102000.

#### References

- [1] S. Jahn, J. Seror, J. Klein, Lubrication of articular cartilage, Annu. Rev. Biomed. Eng. 18 (2016) 235–258.
- [2] A. Cui, et al., Global, regional prevalence, incidence and risk factors of knee osteoarthritis in population-based studies, eClinicalMedicine 29–30 (2020), 100587.
- [3] S. Glyn-Jones, et al., Osteoarthritis, Lancet 386 (2015) 376-387.
- [4] D.J. Hunter, clinical therapeutics viscosupplementation for osteoarthritis of the knee, N. Engl. J. Med. 11 (2015) 1040–1047.
- [5] C.R. Scanzello, S.R. Goldring, The role of synovitis in osteoarthritis pathogenesis, Bone 51 (2012) 249–257.
- [6] J. Sellam, F. Berenbaum, The role of synovitis in pathophysiology and clinical symptoms of osteoarthritis, Nat. Rev. Rheumatol. 6 (2010) 625–635.
- [7] K. S. Osteoarthritis: diagnosis and Treatment, Am. Fam. Physician 85 (2012) 49–56.
- [8] R.D. Altman, A. Manjoo, A. Fierlinger, F. Niazi, M. Nicholls, The mechanism of action for hyaluronic acid treatment in the osteoarthritic knee: a systematic review, BMC Musculoskelet. Disord. 16 (2015) 1–10.

[9] B. Arroll, F. Goodyear-Smith, Corticosteroid injections for osteoarthritis of the knee: meta-analysis, Br. Med. J. 328 (2004) 869–879.

- [10] S.J. Cross, K.E. Linker, F.M. Leslie, Articular cartilage- and synoviocyte-binding poly(ethylene glycol) nano-composite microgels as intra-articular drug delivery vehicles for the treatment of osteoarthritis, ACS Biomater. Sci. Eng. 6 (2020) 5084–5095.
- [11] X.L. Ma, et al., Efficacy and safety of intraarticular hyaluronic acid and corticosteroid for knee osteoarthritis: a meta-analysis, Int. J. Surg. 39 (2017) 95–103
- [12] J. Klein, Chemistry: repair or replacement A joint perspective, Science 323 (2009) 47–48 (80-.).
- [13] G.M. Pontes-Quero, et al., Active viscosupplements for osteoarthritis treatment, Semin. Arthritis Rheum. 49 (2019) 171–183.
- [14] N. Gerwin, C. Hops, A. Lucke, Intraarticular drug delivery in osteoarthritis, Adv. Drug Deliv. Rev. 58 (2006) 226–242.
- [15] C. Li, et al., A review on the wide range applications of hyaluronic acid as a promising rejuvenating biomacromolecule in the treatments of bone related diseases, Int. J. Biol. Macromol. 165 (2020) 1264–1275.
- [16] S. Bowman, M.E. Awad, M.W. Hamrick, M. Hunter, S. Fulzele, Recent advances in hyaluronic acid based therapy for osteoarthritis, Clin. Transl. Med. 7 (2018) 6–17.
- [17] I.S. Bayer, Hyaluronic acid and controlled release: a review, Molecules 25 (2020)
- [18] E.D. Bonnevie, D. Galesso, C. Secchieri, L.J. Bonassar, Frictional characterization of injectable hyaluronic acids is more predictive of clinical outcomes than traditional rheological or viscoelastic characterization, PLoS One 14 (2019) 1–15.
- [19] K. Edsman, et al., Intra-articular duration of Durolane™ after single injection into the rabbit knee, Cartilage 2 (2011) 384–388.
- [20] E.J. Strauss, J.A. Hart, M.D. Miller, R.D. Altman, J.E. Rosen, Hyaluronic acid viscosupplementation and osteoarthritis: current uses and future directions, Am. J. Sports Med. 37 (2009) 1636–1644.
- [21] P. Maudens, S. Meyer, C.A. Seemayer, O. Jordan, E. Allémann, Self-assembled thermoresponsive nanostructures of hyaluronic acid conjugates for osteoarthritis therapy, Nanoscale 10 (2018) 1845–1854.
- [22] F. Cilurzo, et al., Injectability evaluation: an open issue, AAPS PharmSciTech 12 (2011) 604–609.
- [23] Y. Kanazawa, N. De Laurentis, A. Kadiric, Studies of friction in grease-lubricated rolling bearings using ball-on-disc and full bearing tests, Tribol. Trans. 63 (2020) 77–89
- [24] A. Sarkar, F. Kanti, A. Gulotta, B.S. Murray, S. Zhang, Aqueous lubrication, structure and rheological properties of whey protein microgel Particles, Langmuir 33 (2017) 14699–14708.
- [25] B.K. Kim, D.L. Han, K.H. Kang, J. Kim, D.E. Kim, Numerical and experimental study of tribological properties of glass/polymer-based micro ball bearings, Wear 488–489 (2022).
- [26] Y. Duan, Y. Liu, C. Zhang, Z. Chen, S. Wen, Insight into the tribological behavior of liposomes in artificial joints, Langmuir 32 (2016) 10957–10966.
- [27] P. Maudens, O. Jordan, E. Allémann, Recent advances in intra-articular drug delivery systems for osteoarthritis therapy, Drug Discov. Today 23 (2018) 1761–1775.
- [28] Y. Lei, et al., Injectable hydrogel microspheres with self-renewable hydration layers alleviate osteoarthritis, Sci. Adv. 8 (2022).
- [29] Y. Yan, et al., Euryale ferox seed-inspired superlubricated nanoparticles for treatment of osteoarthritis, Adv. Funct. Mater. 29 (2019).
- [30] L. Bedouet, et al., Intra-articular fate of degradable poly(ethyleneglycol)-hydrogel microspheres as carriers for sustained drug delivery, Int. J. Pharm. 2013 (2013) 536–544.
- [31] J.L. Rios, G. Lu, N.E. Seo, T. Lambert, D. Putnam, Prolonged release of bioactive model proteins from anionic microgels fabricated with a new microemulsion approach, Pharm. Res. 33 (2016) 879–892.
- [32] J.M. Pelet, D. Putnam, Poly(acrylic acid) undergoes partial esterification during RAFT synthesis in methanol and interchain disulfide bridging upon NaOH treatment, Macromol. Chem. Phys. 213 (2012) 2536–2540.
- [33] J.M. Petet, D. Putnam, High molecular weight poly(methacrylic acid) with narrow polydispersity by RAFT polymerization, Macromolecules 42 (2009) 1494–1499.
- [34] E. Feeney, et al., Inflammatory and noninflammatory synovial fluids exhibit new and distinct tribological endotypes, J. Biomech. Eng. 142 (2020) 1–10.
- [35] E. Feeney, et al., Temporal changes in synovial fluid composition and elastoviscous lubrication in the equine carpal fracture model, J. Orthop. Res. 37 (2019) 1071–1079.
- [36] E.D. Bonnevie, D. Galesso, C. Secchieri, I. Cohen, L.J. Bonassar, Elastoviscous transitions of articular cartilage reveal a mechanism of synergy between lubricin and hyaluronic acid, PLoS One 10 (2015) 1–15.
- [37] M.E. Fox, F.C. Szoka, J.M.J. Fréchet, Soluble polymer carriers for the treatment of cancer: the importance of molecular architecture, Acc. Chem. Res. 42 (2009) 1141–1151
- [38] L.W. Seymour, R. Duncan, J. Strohalm, J. Kopeček, Effect of molecular weight (Mw) of N-(2-hydroxypropyl)methacrylamide copolymers on body distribution and rate of excretion after subcutaneous, intraperitoneal, and intravenous administration to rats, J. Biomed. Mater. Res. 21 (1987) 1341–1358.
- [39] N.A. Peppas, A.R. Khare, Preparation, structure and diffusional behavior of hydrogels in controlled release, Adv. Drug Deliv. Rev. 11 (1993) 1–35.
- [40] Aetna, Viscosupplementation, 1–88. aetna.com/cpb/medical/data/100\_199/0179. html (2023).
- [41] S.S. Halacheva, et al., Injectable biocompatible and biodegradable pH-responsive hollow particle gels containing poly(acrylic acid): the effect of copolymer composition on gel properties, Biomacromolecules 15 (2014) 1814–1827.

- [42] J.M. Pelet, D. Putnam, An in-depth analysis of polymer-analogous conjugation using DMTMM, Bioconjugate Chem. 22 (2011) 329–337.
- [43] K. Thompson, S. Michielsen, Novel synthesis of N-substituted polyacrylamides: derivatization of poly(acrylic acid) with amines using a triazine-based condensing reagent, J. Polym. Sci. A Polym. Chem. 44 (2006) 126–136.
- [44] M. Kunishima, et al., 4-(4,6-Dimethoxy-1,3,5-triazin-2-yl)-4-methylmorpholinium chloride: an efficient condensing agent leading to the formation of amides and esters, Tetrahedron 55 (1999) 13159–13170.
- [45] M. Kunishima, et al., Esterification of carboxylic acids with alcohols by 4-(4,6-dimethoxy-1,3,5-triazin-2-yl)-4-methyl-morpholinium chloride (DMTMM), Synlett (1999) 1255–1256, https://doi.org/10.1055/s-1999-2828.
- [46] J. Enrione, et al., Rheological and structural study of salmon gelatin with controlled molecular weight, Polymers 12 (2020) 1–17 (Basel).
- [47] C.P.J. Wong, P. Choi, Prediction of crossover in the molecular weight dependence of polyethylene viscosity using a polymer free volume theory, Soft Matter 16 (2020) 7458–7469.
- [48] S.G. Cook, L.J. Bonassar, Interaction with cartilage increases the viscosity of hyaluronic acid solutions, ACS Biomater. Sci. Eng. 6 (2020) 2787–2795.
- [49] N.A. Peppas, P. Bures, W. Leobandung, H. Ichikawa, Hydrogels in pharmaceutical formulations, Eur. J. Pharm. Biopharm. 50 (2000) 27–46.
- [50] J.T. Peters, M.E. Wechsler, N.A. Peppas, Advanced biomedical hydrogels: molecular architecture and its impact on medical applications, Regen. Biomater. 8 (2021) 1–21.
- [51] M.E. Wechsler, et al., Engineered microscale hydrogels for drug delivery, cell therapy, and sequencing, Biomed. Microdevices 21 (2019) 31–46.
- [52] M.M. Temple-Wong, et al., Hyaluronan concentration and size distribution in human knee synovial fluid: variations with age and cartilage degeneration, Arthritis Res. Ther. 18 (2016) 1–8.
- [53] K. Zhang, et al., Thermo-Sensitive Dual-Functional Nanospheres with Enhanced Lubrication and Drug Delivery for the Treatment of Osteoarthritis, Chem. A Eur. J. 26 (2020) 10564–10574.
- [54] W. Li, et al., Biodegradable lubricating mesoporous silica nanoparticles for osteoarthritis therapy, Friction 10 (2020) 68–79.
- [55] H. Chen, et al., Cartilage matrix-inspired biomimetic superlubricated nanospheres for treatment of osteoarthritis, Biomaterials 242 (2020) 1–17.
- [56] Q. Chen, et al., Semi-interpenetrating network hyaluronic acid microgel delivery systems in micro-flow, J. Colloid Interface Sci. 519 (2018) 174–185.
- [57] J.J. Stickel, R.L. Powell, Fluid mechanics and rheology of dense suspensions, Annu. Rev. Fluid Mech. 37 (2005) 129–149.
- [58] A. Einstein, Investigations on the theory of the brownian movement, Ann. d. Phys. 17 (1905) 549–567.
- [59] G.K. Batchelor, J.T. Green, The determination of the bulk stress in a suspension of spherical particles to order c2, J. Fluid Mech. 56 (1972) 401–427.
- [60] I.M. Krieger, T.J. Dougherty, A mechanism for non-newtonian flow in suspensions of rigid spheres. Trans. Soc. Rheol. 3 (1959) 137–152.
- [61] G. Liu, M. Cai, F. Zhou, W. Liu, Charged polymer brushes-grafted hollow silica nanoparticles as a novel promising material for simultaneous joint lubrication and treatment, J. Phys. Chem. B 118 (2014) 4920–4931.
- [62] L. Yang, et al., Synthesis of charged chitosan nanoparticles as functional biolubricant, Colloids Surf. B Biointerfaces 206 (2021) 1–7.

[63] Y. Han, et al., Biomimetic injectable hydrogel microspheres with enhanced lubrication and controllable drug release for the treatment of osteoarthritis, Bioact. Mater. 6 (2021) 3596–3607.

Materialia 33 (2024) 102000

- [64] J. Yang, et al., Ball-bearing-inspired polyampholyte-modified microspheres as biolubricants attenuate osteoarthritis, Small 16 (2020).
- [65] P. Anilkumar, et al., Mega macromolecules as single molecule lubricants for hard and soft surfaces, Nat. Commun. 11 (2020).
- [66] A. Singh, et al., Enhanced lubrication on tissue and biomaterial surfaces through peptide-mediated binding of hyaluronic acid, Nat. Mater. 13 (2014) 988–995.
- [67] M. Wathier, et al., A large-molecular-weight polyanion, synthesized via ringopening metathesis polymerization, as a lubricant for human articular cartilage, J. Am. Chem. Soc. 135 (2013) 4930–4933.
- [68] Z. Sun, et al., Boundary mode lubrication of articular cartilage with a biomimetic diblock copolymer, Proc. Natl. Acad. Sci. U. S. A. 116 (2019) 12437–12441.
- [69] K. Vishwanath, S.R. McClure, L.J. Bonassar, Polyacrylamide hydrogel lubricates cartilage after biochemical degradation and mechanical injury, J. Orthop. Res. 41 (2022) 1–9
- [70] J.P. Gleghorn, L.J. Bonassar, Lubrication mode analysis of articular cartilage using stribeck surfaces, J. Biomech. (2008), https://doi.org/10.1016/j. ibiomech.2008.03.043.
- [71] D.L. Burris, L. Ramsey, B.T. Graham, C. Price, A.C. Moore, How sliding and hydrodynamics contribute to articular cartilage fluid and lubrication recovery, Tribol. Lett. 67 (2019) 46–56.
- [72] L. Shi, V.I. Sikavitsas, A. Striolo, Experimental friction coefficients for bovine cartilage measured with a pin-on-disk tribometer: testing configuration and lubricant effects, Ann. Biomed. Eng. 39 (2011) 132–146.
- [73] E.D. Bonnevie, et al., Sub-critical impact inhibits the lubricating mechanisms of articular cartilage, J. Biomech. 53 (2017) 64–70.
- [74] E.D. Bonnevie, D. Galesso, C. Secchieri, L.J. Bonassar, Degradation alters the lubrication of articular cartilage by high viscosity, hyaluronic acid-based lubricants, J. Orthop. Res. 36 (2018) 1456–1464.
- [75] B.A. Lakin, et al., A synthetic bottle-brush polyelectrolyte reduces friction and wear of intact and previously worn cartilage, ACS Biomater. Sci. Eng. 5 (2019) 3060–3067.
- [76] D. Rebenda, et al., Rheological and frictional analysis of viscosupplements towards improved Jubrication of human joints. Tribol. Int. 160 (2021).
- [77] L. Ma, A. Gaisinskaya-Kipnis, N. Kampf, J. Klein, Origins of hydration lubrication, Nat. Commun. 6 (2015) 8–13.
- [78] N.L. Cuccia, S. Pothineni, B. Wu, J.M. Harper, J.C. Burton, Pore-size dependence and slow relaxation of hydrogel friction on smooth surfaces, Proc. Natl. Acad. Sci. U. S. A. 117 (2020) 11247–11256.
- [79] J.P. Gong, Friction and lubrication of hydrogels Its richness and complexity, Soft Matter 2 (2006) 544–552.
- [80] C. Larsen, et al., Intra-articular depot formulation principles: role in the management of postoperative pain and arthritic disorders, J. Pharm. Sci. 97 (2008) 4622–4654.
- [81] R. Altman, J. Hackel, F. Niazi, P. Shaw, M. Nicholls, Efficacy and safety of repeated courses of hyaluronic acid injections for knee osteoarthritis: a systematic review, Semin. Arthritis Rheum. 48 (2018) 168–175.